Preprints (www.preprints.org) | NOT PEER-REVIEWED | Posted: 3 February 2021 doi:10.20944/preprints202102.0118.v1

Effective removal of Amido black and Eosin B dyes in aqueous solution by MWCNT/ZrO_2/Pb nanocomposites: Isotherm, reusability and kinetic studies

Marjan Sheibani [1], Mehrorang Ghaedi [2, *], Vahid Zare-Shahabadi [1] and Arash Asfaram [3]

[1] *Department of Chemistry, Mahshahr Branch, Islamic Azad University, Mahshahr, Iran*
[2] *Department of Chemistry, Yasouj University, Yasouj 75918-74831, Iran.*
[3] *Medicinal Plants Research Center, Yasuj University of Medical Sciences, Yasuj, Iran*

Abstract

This research illustrates modification of multi-walled carbon nanotubes (MWCNT) by ZrO_2/Pb to construct nanocomposites (MWCNT/ZrO_2/Pb-NCs) by simple precipitation technique and subsequently examine its ability for adsorption of Amido black (AB) and Eosin B (EB) dyes in binary system. The present nanocomposites investigation by FESEM, XRD, FTIR, and EDX analysis, reveal its as-synthesized crystalline nature with cubic morphology and average particle size 30–50 nm. The present nano-adsorbent represent high efficiency for AB and EB adsorption from aqueous solution, while dependency of variables including pH, initial concentration of dyes, contact time and MWCNT/ZrO_2/Pb-NCs mass were analyzed by central composite design (CCD). The predicted maximum removal percentage was 95% removal for both dyes is consequence of adjustment of operational conditions at pH of 6.0; 0.05 g MWCNT/ZrO_2/Pb-NCs; 15 min stirring at 15 mg L^{-1} for both dyes. The Langmuir as applicable for representation and description of reveal data of adsorption with adsorption capacity of 15.46 and 16.92 mg g^{-1} for AB and EB, respectively. Pseudo-first order model owing to its high correlation coefficient and closeness of experimental and theoretical data well represented behavior of corresponding adsorption system. Mechanism examination strongly proof high contribution of external mass transference as the main rate-controlling step. The successful regeneration of MWCNT/ZrO_2/Pb-NCs suggested their usefulness in wastewater treatment and its ability of environmental management.

Keywords: Adsorption; Amido black (AB); Central composite design (CCD) ; Eosin B (EB); MWCNT/ZrO_2/Pb-NCs.

* Corresponding author. m_ghaedi@mail.yu.ac.ir (M. Ghaedi)

Preprints (www.preprints.org) | NOT PEER-REVIEWED | Posted: 3 February 2021 doi:10.20944/preprints202102.0118.v1

1. Introduction

Among various activities textile industry attain more attention of applicability owing to dyes for coloration of fiber [1]. Dyes as chemical compounds can migrate to surfaces or fabrics to impart color [2], while their complex organic molecules which according are resistant to heat, light and even oxidation [3]. The effluents containing dyes assumes at polluted resources. Dyes are broadly classified as anionic, cationic, non-ionic and zwitterionic depending on their ionic charge [4].

Most dyes owing to their non-oxidizable nature by traditional biological and physical treatment which emerged from drawbacks like biological oxygen demand and generation of huge amount of wastes [5, 6].

Adsorption as alternative due to its vital role attain great practical environmental technology (mainly in water and wastewater treatment) due to several advantages such as high efficiency, simple operation and easy recovery/reuse of adsorbent [7-9].

Carbon nanotubes base on rolled up graphene sheets, which can be present as single-walled (SWCNT) or multiwalled (MWCNT) depending on their preparation conditions These tubes consist of [10, 11]. Their exceptional mechanical properties, unique electrical properties, high chemical and thermal stability and a large specific surface area are motivation for great attention in latent applications such as composite reinforcement [12-14].

Owing to their surface functional groups and hydrophobic surfaces candidate such material for interactions and bonding heavy metal ions as well as organic compounds [15-17]. Thus, nanoparticles deposited and/or decorated on the MWCNTs to generate useful adsorbents for accumulation and elimination of organic compounds.

Owing to combination of different materials to supply fantastic features MWCNTs–ZrO have attain great interest to benefit integrated properties of MWCNTs which modified with ZrO, Pb. It is therefore anticipated that the modification of MWCNTs with ZrO_2 and Pb and generation of hybrid nanocomposite supply excellent adsorption property via generation of subsequent functional groups.

MWCNTs as adsorbent in our research group was exclusively carried out in single dye adsorption [18-20] in continue some researches were undertaken on binary systems [21] Multiple components and multiplicity may affect dyes adsorption behavior, while owing to competitive adsorption lead to lower dyes adsorption.

One major challenge for the utilization of removal techniques is finding best operational conditions to provide acceptable response at low content of adsorbent [22]. Hence, central composite design (CCD) useful approach is applicable to examine the effects of several factors as main and interaction part following their simultaneous changing and performing a limited number of experiments [23]. 2^4 small factorial CCD applied to check the combined effect of pH, MWCNT/ZrO_2/Pb-NCs mass, dyes concentration and contact time on two under study Amido black (AB) and Eosin B (EB) dyes dyes adsorption by a MWCNT/ZrO_2/Pb-NCs.

In this study amido black and eosine B with abundant application in some or part of chemical, textile, paper industries, biological stain, paints, inks, plastics, and leather industries was selected as model pollutant to evaluate parameters about their adsorption kinetics and thermodynamics onto MWCNT/ZrO_2/Pb-NCs under different experimental conditions such as the effect of AB and EB concentration, adsorbent mass, pH, and contact time. Kinetics and isotherm data appropriately wee fitted by Langmuir and pseudo second order kinetic model.

Preprints (www.preprints.org) | NOT PEER-REVIEWED | Posted: 3 February 2021 doi:10.20944/preprints202102.0118.v1

2. Materials and methods

2.1. Chemicals, reagents and instruments

All chemicals and reagents (analytical grade) supplied from Merck, Darmstadt, Germany and distilled water was used thorough out solutions preparation. The 200 mg L^{-1} stock solutions of under study dyes were prepared by dissolving 20 mg of AB and/or EB in 100 mL of distilled water and subsequently were diluted daily to supply solution in the range of 1–50 mg L^{-1} .

2.2. Preparation of MWCNT/ZrO_2/Pb-NCs

1 g MWCNTs was dispersed in 50 mL of distilled water and in the presence of ultrasonic stirred for 30 min, then 0.7 g of terephthalic acid and 3.5 g of $ZrO(NO_3)_2.6H_2O$ were added to the above solution and subsequently 10 mL mixture of DMF: ethanol (50:50v/v%) were added to above solutions and subsequently sonicated for 30 min and the mixture was autoclave at 160 °C for 18 h, calcined at 350 °C for 2 h, respectively. 1 g of products were dispersed in 80 ml of acetonitrile and 0.035 g of Pb-NPs was added and subsequently stirred for 60 min at room temperature and after filtering, washing (several times) by ethanol and final draying at 70 °C for 3 h was applied for understudy dyes removal. All the instruments for the characterization fully described previously[24-26].

2.3. Batch experiments

The batch experiments were undertaken according to our conventional approach at 50 mL of AB and EB (1-15 mg L^{-1}), 0.02-0.05 g of MWCNT/ZrO_2/Pb-NCs following stirring 2-18 min at pH 4.0-8.0 and room temperature. After predetermined time intervals, the solutions were taken out and centrifuged. The standard deviations for all the parameters ranged from 1.0 to 1.5%. and in all experiments points, the magnitude of non-adsorbed content of AB and EB was quantified according curve supplied at the same conditions and their adsorption capacity (mg g^{-1}) was calculated using the following equation [27]:

$$q_e = \frac{(C_0 - C_e)V}{M} \quad (1)$$

where q_e = the Amido black and Eosin B dyes concentration on the adsorbent at equilibrium (mg of each dyes/g of MWCNT/ZrO_2/Pb-NCs), C_0 = the initial each dyes concentration in the liquid phase (mg of dye L^{-1}), C_e = the liquid-phase dyes concentration at equilibrium (mg of each dyes L^{-1}), V = the total volume of dye- MWCNT/ZrO_2/Pb-NCs mixture, and M = mass of MWCNT/ZrO_2/Pb-NCs used (g). The AB and EB adsorption was calculated based on following equation [28].

$$\%\text{adsorption} = \left(\frac{C_0 - C_e}{C_0}\right) \times 100\% \quad (2)$$

2.4. Experimental design

(CCD [29, 30] applied to investigate effect of contact time (X_1), the AB (X_2) and EB (X_3) content, and the MWCNT/ZrO_2/Pb-NCs mass (X_4) were chosen as the independent variables. The adsorption percentage of two dyes was chosen as the dependent output responses variables. Each factor was examined at five levels, coded −2, −1, 0, +1 and +2, as shown in **Table 1** following conduction of 20 experiments. The actual experimental design matrix (**Table 2**) is applied to represent and estimate coefficient of determination (R^2), Pareto chart, analysis of variance (ANOVA) statistical and response plots to judge about significant terms, main of effect and interactions.

Preprints (www.preprints.org) | NOT PEER-REVIEWED | Posted: 3 February 2021 doi:10.20944/preprints202102.0118.v1

Table. 2. Analysis of variance (ANOVA) for fit of adsorption of Amido black and Eosin B dyes from central composite design.

Source of variation	*Df*[a]	**R % Amido black**					**R % Eosin B**			
		SS[b]	*MS*[c]	*F-value*	*P-value*		*SS*	*MS*	*F-value*	*P-value*
Model	14	7255	518.2	52.38	0.000183		1.05E+04	749	60.51	0.000128
X_1	1	686.7	686.7	69.41	0.000407		639.7	639.7	51.69	0.000811
X_2	1	1788	1788	180.7	< 0.0001		188.2	188.2	15.2	0.01142
X_3	1	670.2	670.2	67.74	0.000431		4928	4928	398.1	< 0.0001
X_4	1	1350	1350	136.4	< 0.0001		2490	2490	201.2	< 0.0001
X_1X_2	1	41.63	41.63	4.208	0.09548		80.78	80.78	6.526	0.05098
X_1X_3	1	7.201	7.201	0.7278	0.4325		5.595	5.595	0.452	0.5312
X_1X_4	1	7.304	7.304	0.7382	0.4295		0.104	0.104	0.0084	0.9305
X_2X_3	1	95.98	95.98	9.701	0.02641		24.19	24.19	1.954	0.221
X_2X_4	1	627.9	627.9	63.46	0.000503		310.2	310.2	25.06	0.004083
X_3X_4	1	58.27	58.27	5.889	0.05962		118.5	118.5	9.574	0.02703
X_1^2	1	55.12	55.12	5.571	0.06473		109.5	109.5	8.85	0.03098
X_2^2	1	156.3	156.3	15.8	0.01059		104.2	104.2	8.417	0.03374
X_3^2	1	8.558	8.558	0.865	0.395		355.9	355.9	28.76	0.003033
X_4^2	1	171.1	171.1	17.29	0.008837		304.9	304.9	24.63	0.004236
Residual	5	49.47	9.894				61.89	12.38		
Lack of Fit	2	7.057	3.528	0.2496	0.7939		6.882	3.441	0.1877	0.8379
Pure Error	3	42.41	14.14				55	18.33		
Corr Total	19	7304					1.06E+04			

Statistical parameters obtained from the analysis of variance for the reduced models

Response	*Standard Deviation (SD)*	*Mean*	*Coefficient of Variance (C.V. %)*	R^2	*Adj-R^2*	*Pred-R^2*	*Adequate precision (AP)*
R% Amido black	3.145	70.47	4.463	0.993	0.974	0.939	24.67
R% Eosin B	3.518	64.14	5.485	0.994	0.978	0.961	23.84

Preprints (www.preprints.org) | NOT PEER-REVIEWED | Posted: 3 February 2021 doi:10.20944/preprints202102.0118.v1

Table. 1. Independent variables and their levels for the central composite design used in the present study

Independent variables			Range and levels (coded)				
Factors	Coded	Units	-α (-2.0)	Low (-1)	Center (0)	High (+1)	+α (+2.0)
Contact time	X_1	min	2.00	6.00	10.00	14.00	18.00
AB concentration	X_2	mg L^{-1}	5.00	10.00	15.00	20.00	25.00
EB concentration	X_3	mg L^{-1}	5.00	10.00	15.00	20.00	25.00
Adsorbent mass	X_4	g	0.020	0.030	0.040	0.050	0.060

Run order	Adsorption variables				Response	
	X_1	X_2	X_3	X_4	R % Amido black (AB)	R % Eosin B (EB)
1	14	10	10	0.05	90.00	91.30
2	18	15	15	0.04	88.54	83.00
3	6	20	20	0.05	63.00	53.00
4	10	15	15	0.04	74.20	71.70
5	10	15	15	0.06	91.30	94.60
6	2	15	15	0.04	51.48	47.23
7	10	15	15	0.04	78.20	74.92
8	6	10	20	0.03	72.20	31.86
9	6	20	10	0.05	74.36	86.80
10	10	15	15	0.02	39.34	24.03
11	10	15	5	0.04	87.90	92.00
12	6	10	10	0.03	80.50	74.10
13	14	20	10	0.03	55.60	66.80
14	14	10	20	0.05	88.70	67.80
15	10	15	15	0.04	80.80	68.90
16	10	15	15	0.04	72.53	78.85
17	14	20	20	0.03	29.65	20.95
18	10	5	15	0.04	95.70	75.03
19	10	15	25	0.04	59.58	24.30
20	10	25	15	0.04	35.90	55.63

3. Results and discussion

3.1. Characteristics of synthesized MWCNT/ZrO_2/Pb-NCs

Fourier transform infrared spectroscopic analysis (FTIR) of MWCNT/ZrO_2/Pb-NCs(**Fig. 1),** confirms the defective sites at the surface of MWCNT/ZrO_2/Pb-NCs and the presence of O-H group (3413 cm^{-1}), C-H group (2923 cm^{-1}), C=C (1619 cm^{-1}1), C-C (1348 cm^{-1}) and C-O group (1120 cm^{-1}) functional groups at the surface of MWNTs [31]. In addition, strong bands over from 485 to 619 cm^{-1} is probably assign to the presence of a Zr-O bond.

Preprints (www.preprints.org) | NOT PEER-REVIEWED | Posted: 3 February 2021 doi:10.20944/preprints202102.0118.v1

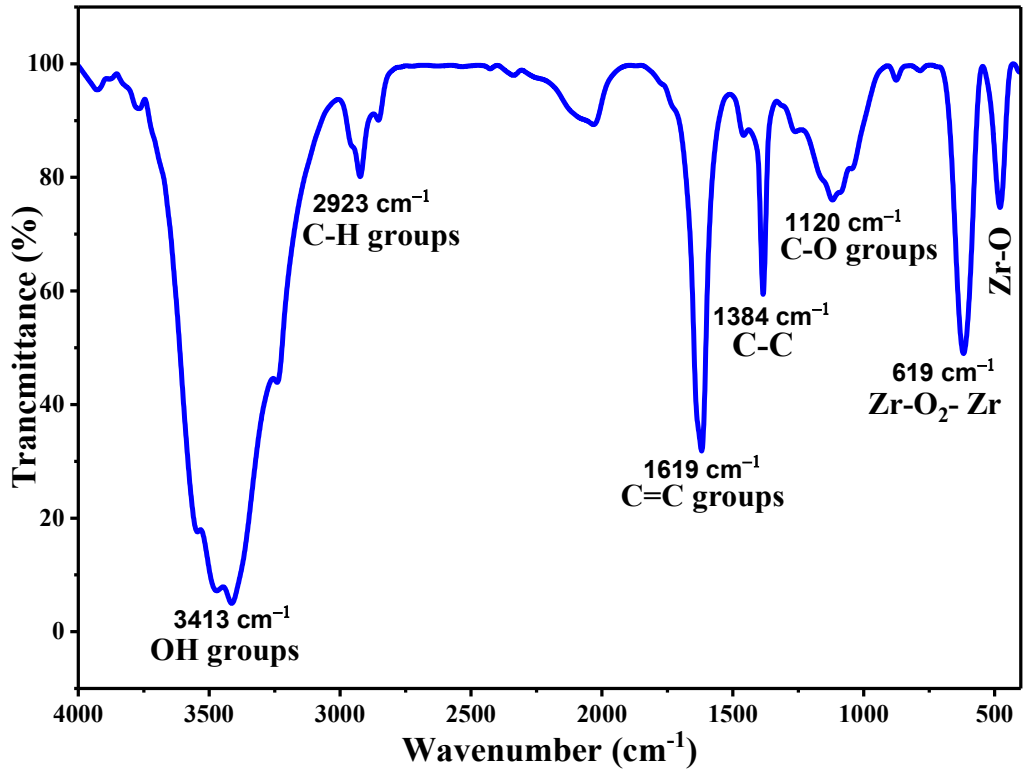

Fig. 1. FTIR spectrum of MWCNT/ZrO2/Pb-NCs.

The crystallographic nature of the MWCNT/ZrO_2/Pb-NCs investigated by XRD analysis (**Fig. 2**) reveals the typical peaks of MWCNTs at 2θ = 25.91° (JCPDS NO. 96-900-1992) while simultaneously appearance of diffraction peaks at 2θ values of 31.20° (111), 34.2° (020), 50.02° (12-2), and 55.89 (031) proof successful formation of ZrO_2 (JCPDS NO. 96–101–0913). The diffraction peaks at 2θ values of 31.20° (111), and 79.20 (222) related to Pb (JCPDS NO. 96-901-3419) are clearly seen in the purified MWCNT/ZrO_2/Pb-NCs. The results confirm that ZrO_2/Pb nanoparticles encapsulated into the interiors of MWCNTs or adsorbed on the surface of MWCNTs.

Preprints (www.preprints.org) | NOT PEER-REVIEWED | Posted: 3 February 2021 doi:10.20944/preprints202102.0118.v1

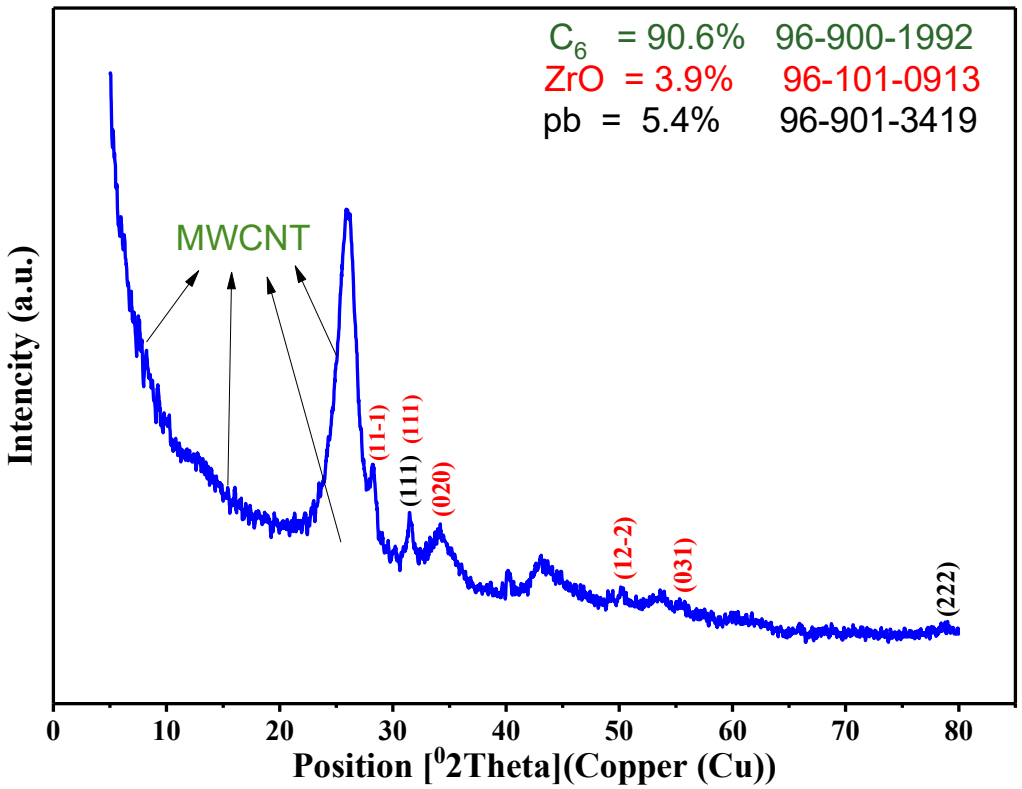

Fig. 2. XRD patterns of MWCNT/ZrO_2/Pb-NCs.

The FESEM images of MWCNT/ZrO_2/Pb-NCs (**Fig. 3a-c**), illustrate ZrO_2/Pb particles take place in the cluster form on the MWCNT sidewalls (**Fig. 3a-b**), while the diameter of MWCNT and ZrO_2/Pb particles is in the range of 20–30 nm and 30–55 nm, respectively. This evidence proof occurrence and accumulation of some part of ZrO_2/Pb onto surface of MWCNTs.

The chemical composition of the ZrO_2/Pb nanoparticles inside MWCNT was analyzed by EDX (**Fig. 3d**) shows Zr, O, C and Pb. It is obvious that the Zr and Pb peak is caused by the ZrO_2/Pb grid used to clamp the nanoparticles., while carbon comes from MWCNT. EDX quantitative microanalysis indicates the presence of carbon (92.4%), oxygen (0.01%), zirconium (2.59%) and lead (5.0%) in the MWCNT/ZrO_2/Pb-NCs.

Preprints (www.preprints.org) | NOT PEER-REVIEWED | Posted: 3 February 2021 doi:10.20944/preprints202102.0118.v1

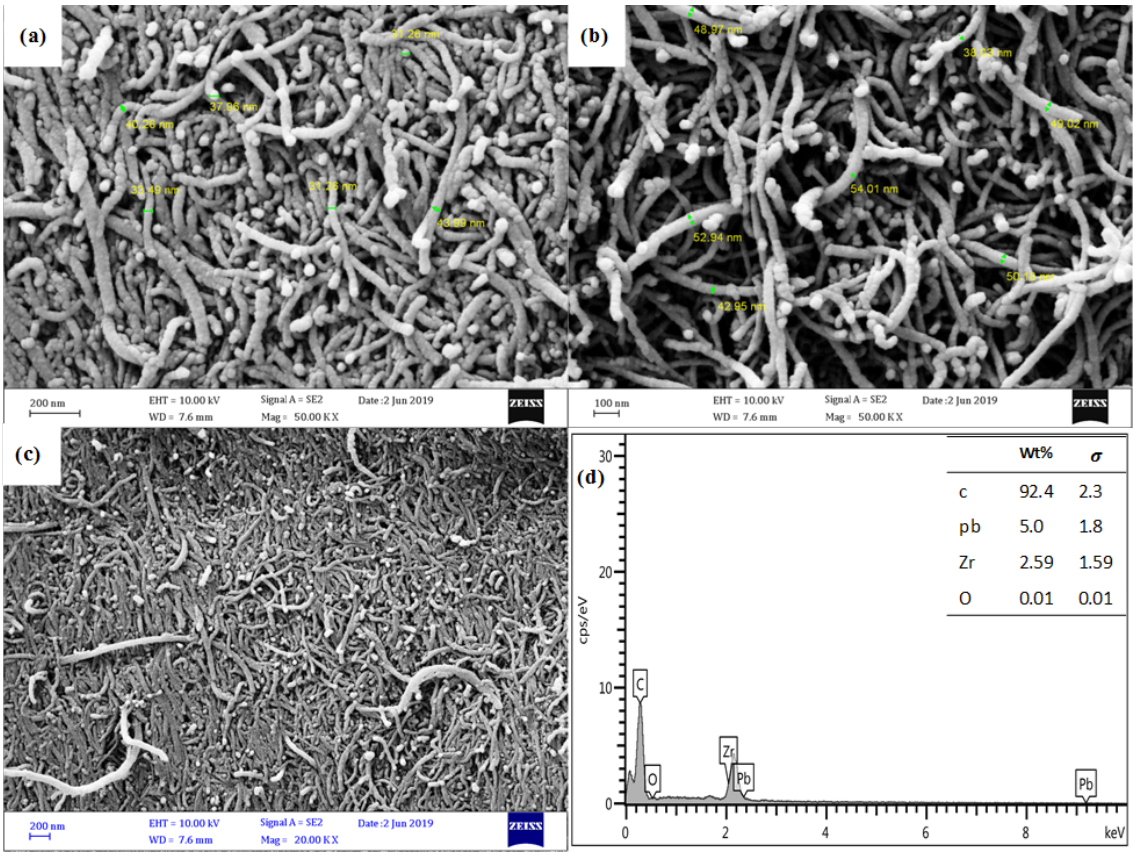

Fig. 3. Typical FESEM images (a-c) and EDX (d) of the MWCNT/ZrO_2/Pb-NCs.

3.2. Concentration measurement and calibration

Calibration curve (**Fig. 4**) and zero absorbance spectra of single and binary solutions of AB and EB dyes at 15 mg L^{-1} (**Fig. 5**) show that their separate absorbance peaks significantly differ from their binary solution at in the same conditions. In this case, violation of Beer–Lambert rule and significant overlap among peaks were take place which is proportional with decreasing the accuracy and repeatability of quantification stage, while present problem to high extent can be lower or eliminated by derivative spectrometry which highly recommended due to its simplicity and easy operation. Moreover, differentiation procedure often produces a high level of noise especially at higher order of derivatives. The zero and first order derivative absorption spectra (**Figs. 5** and **6**) of AB and EB in single and binary mixture (with wavelength) and their zero order derivative spectra in binary mixture reveal ability of acceptable monitoring AB at 621 nm in the presence of Eosin B (**Figs. 6 and 7**), while EB quantified at 497 nm in the presence of AB in first order derivative (**Figs. 6 and 7**). An excellent linear relationship between amplitude $^1D_{621}$, $^1D_{497}$ and respective AB and EB concentration with high correlation coefficient (R^2 > 0.9995) was established in the concentration range of 1-25 mg L^{-1} (**Fig. 7**). The accuracy and precision of constructed calibration curves for AB and EB were checked owing to recovery>94% and RSD<5%.

Preprints (www.preprints.org) | NOT PEER-REVIEWED | Posted: 3 February 2021 doi:10.20944/preprints202102.0118.v1

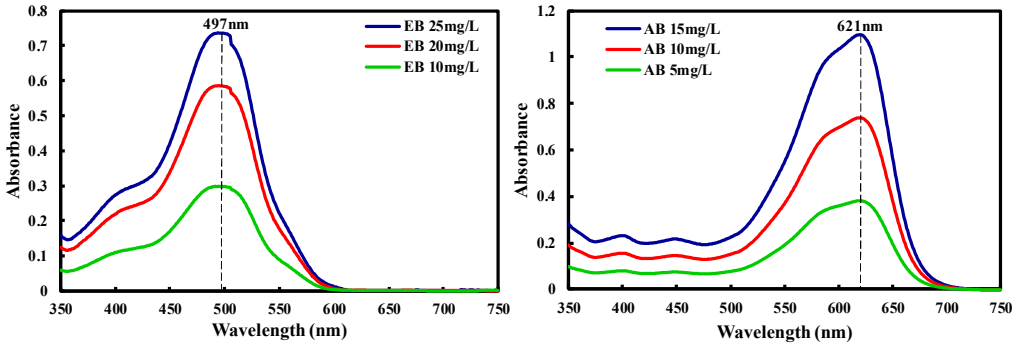

Fig. 4. Zero order absorption spectra Amido black and Eosin B dyes in single solution.

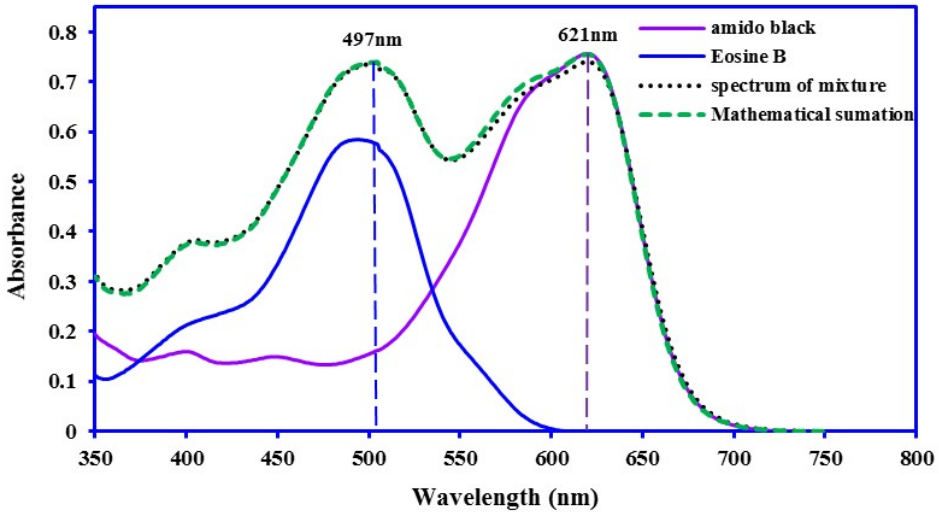

Fig. 5. zero order absorption spectra Amido black and Eosin B dyes in single and binary solution.

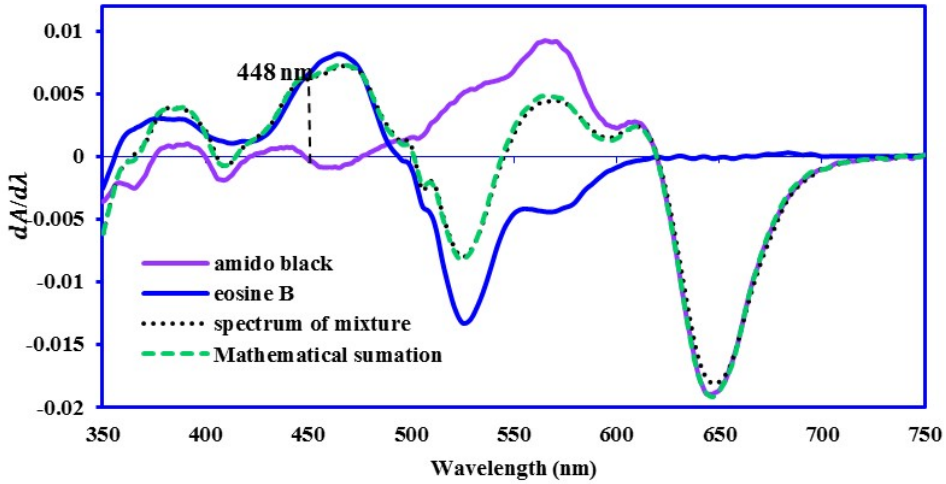

Fig. 6. First order absorption spectra Amido black and Eosin B dyes in binary solution.

Preprints (www.preprints.org) | NOT PEER-REVIEWED | Posted: 3 February 2021 doi:10.20944/preprints202102.0118.v1

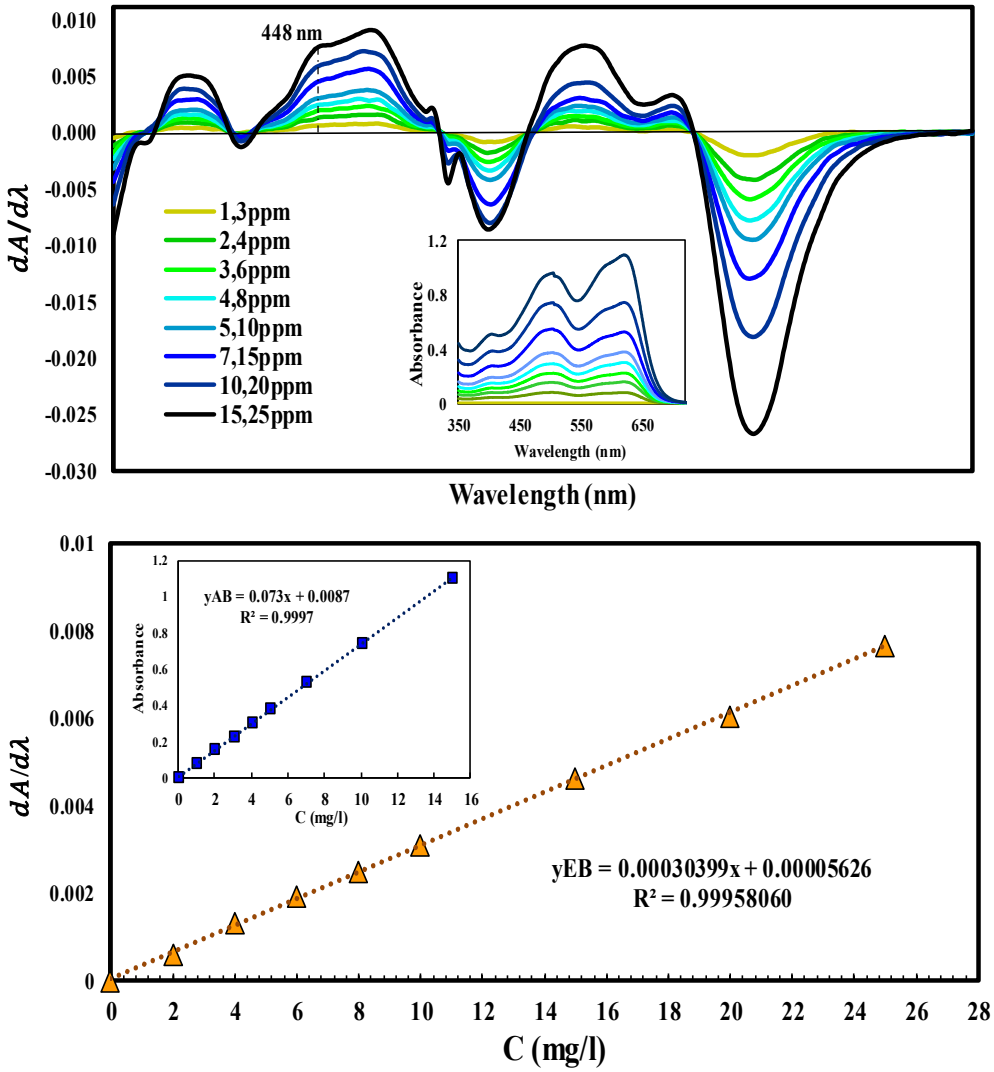

Fig. 7. Calibration curve of the first order derivative spectrophotometry for both dye.

Preprints (www.preprints.org) | NOT PEER-REVIEWED | Posted: 3 February 2021 doi:10.20944/preprints202102.0118.v1

3.3. Effect of pH

The pH with great role on AB and EB adsorption process were examined over pH of 4.0-8.0 (**Fig. 8**) and accordingly respective results proof that AB and EB adsorption was affected by changing pH, while their maximum adsorption was occur at pH of 4.0-6.0.

In the acidic to neutral solutions is associated with generation of positive charge along the MWCNT/ZrO_2/Pb-NCs had positively charged surface, and strongly attain negative charge at basic solutions. Therefore, acidic to neutral media is associated with higher mass transfer of AB and EB on the MWCNT/ZrO_2/Pb-NCs owing to electrostatic interaction.

The pH of zero point of charge (pH_{zpc}), by solid addition method was found approximately at to be 6.8 (**Fig. 8**) and as expected confirm appearance of positive charge over 4.0-6.0 on MWCNT/ZrO_2/Pb-NCs which consequently favored adsorption of both anionic dyes at lower ($pH > pH_{zpc}$), while anionic dye will be favored at low pH ($pH < pH_{zpc}$). Reversely at around 8.0-9.0 as consequence of the surface deprotonation and appearance of negative charge on adsorption lead to hinder from both AB and ED adsorption owing to electrostatic repulsion.

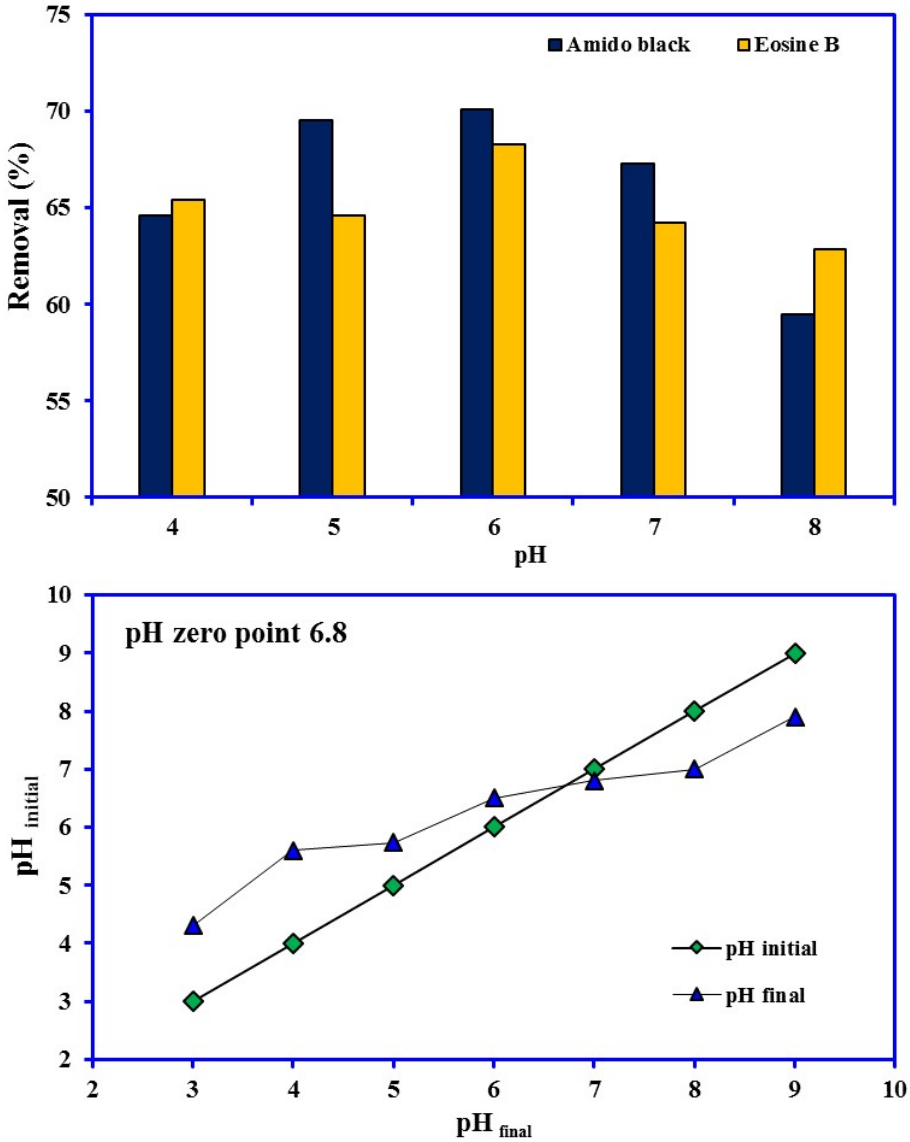

Fig. 8. Effect of the initial pH on the adsorption of two dyes and Point of zero charge of the MWCNT/ZrO_2/Pb-NCs.

Preprints (www.preprints.org) | NOT PEER-REVIEWED | Posted: 3 February 2021 doi:10.20944/preprints202102.0118.v1

3.4. CCD analysis

Analysis of variance (**Table 2**) for the response surface quadratic model represent F-values of 52.38 and 60.51, R^2 of 0.993 and 0.994, probability of <0.0001 and coefficient of variation of 4.463 and 5.485% for AB and EB, respectively, which proof the models are highly significant and the experiments are accurate and reliable. An adequate precision of 24.67 for AB and 23.84 for EB also represent and confirm validity of the models. The lack of fit analysis was found to be non-significant in the present cases. Among all the terms, the linear effects of contact time (X_1), the AB (X_2) and EB (X_3) concentration, and the adsorbent mass (X_4) for two dyes were found to be significant since the p-values were <0.0001 (**Fig. 9**). Similarly, X_2X_4 was found to be the most significant interaction factor owing to the p-value of <0.005. All the quadratic terms, viz., X_2^2 and X_4^2 for Amido black, X_1^2, X_2^2, X_3^2 and X_4^2 for Eosin B were found to be significant owing to their high F-values and low p-values. The other term coefficients were not significant ($P > 0.05$) and based on statistical significance **Eqs. (3 and 4)** can be written as:

$$R\%_{\text{Amido black}} = 138.9 + 3.9X_1 - 9.5X_2 - 0.2X_3 - 762.3X_4 - 0.14X_2X_3 + 250.6X_2X_4 - 0.1X_2^2 - 27111X_4^2 \quad (3)$$

$$R\%_{\text{Eosin B}} = 96.73 + 1.1X_1 - 6.9X_2 - 1.3X_3 + 903.7X_4 + 0.23X_1X_2 + 176.1X_2X_4 + 77.0X_3X_4 - 0.14X_1^2 - 0.09X_2^2 - 0.16X_3^2 - 36200X_4^2 \quad (4)$$

Predicted R^2 is a measure of quality of fitting and ability of model to predicts response value. The adjusted R^2 and predicted R^2 should be within approximately 0.20 of each other to be in reasonable agreement [32] and their difference represent problem along either the data or the model. accordingly, the predicted R^2 of 0.9743 and 0.9777 is in reasonable agreement with the adjusted R^2 of 0.9394 and 0.9609 for AB and EB, respectively.

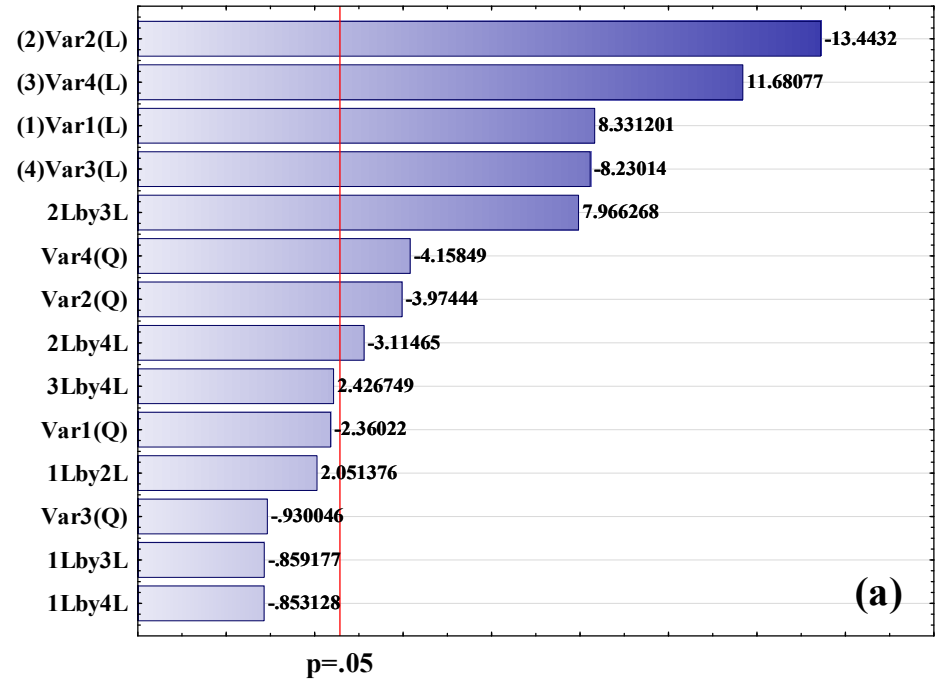

Preprints (www.preprints.org) | NOT PEER-REVIEWED | Posted: 3 February 2021 doi:10.20944/preprints202102.0118.v1

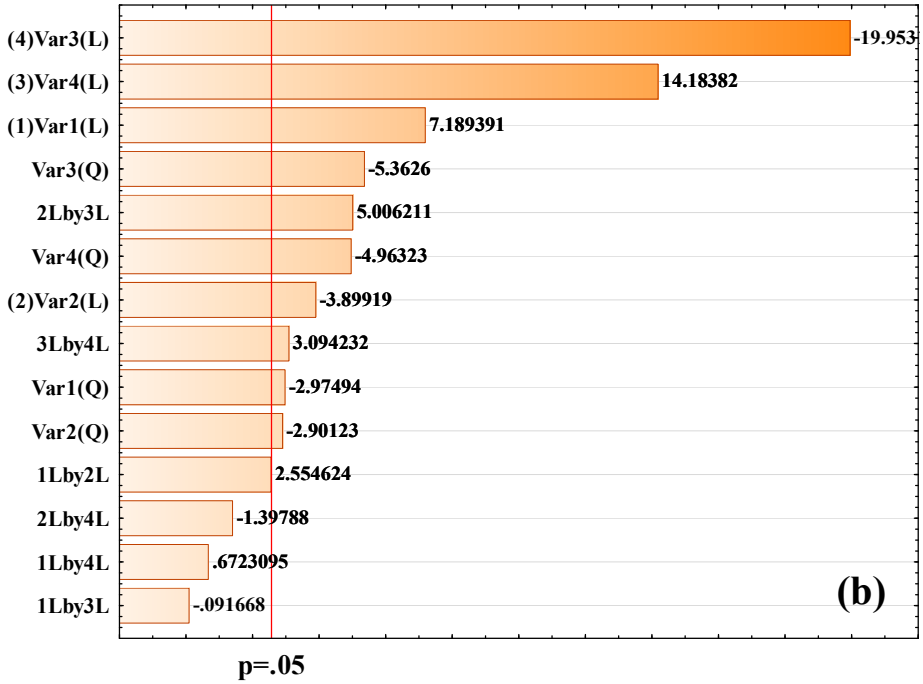

Fig. 9. (a, b) Standardized Pareto chart showing the effect of different factor terms on dyes adsorption values.

3.5. Effect of various parameters on AB and EB removal efficiency

RSM results in the form of 3-D plots and contours (**Fig. 10**a) shows that increasing adsorbent value from 0.02 to 0.06 g at hold and fixed concentration and pH constant (15.0 mg L^{-1} and 6.0), respectively, lead to enhance in percentage from 25.3% to 96.8%. The increase in adsorption value for this situation might be due to availability of more surface area with more functional groups at a higher mass of adsorbent.

Adsorption time with positive significant factor was also the second important factor in the adsorption step. An equilibration time of about 15 min was required for both understudy AB and EB quantitative removal from aqueous solution (**Fig. 10 b, c**).

Combined effect of dyes concentration has been analyzed from the CCD model (**Fig. 10b, c and d**) and reveal higher AB and EB concentration from 5 to 25 mg L^{-1} (keeping other factors constant) is associated reduction in their removal extent from 80% to 15% which might be due to lower ratio of available surface to available dyes molecular by increasing AB and EB content which according reduce their removal percentage, while reverse trend (higher removal percentage) was achieved at lower AB and EB content.

Preprints (www.preprints.org) | NOT PEER-REVIEWED | Posted: 3 February 2021 doi:10.20944/preprints202102.0118.v1

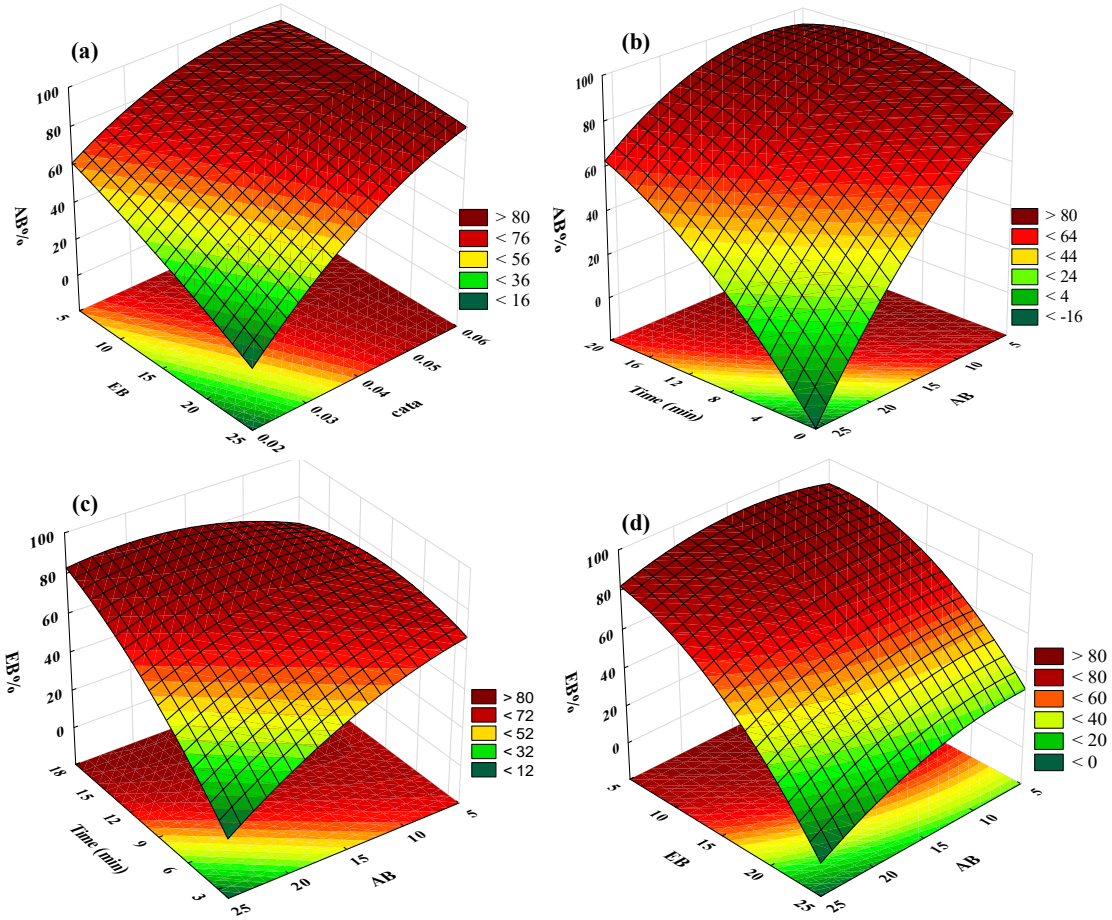

Fig. 10. 3D surface plots indicating interaction effects of independent variables on variation of R%: (a) X_3–X_4 (AB); (b) X_1–X_2 (AB); (c) X_1–X_2 (EB) and (d) X_2–X_3 (EB).

3.6. Selection of optimal levels

The under study work is devoted to examination of adsorption behavior of AB and EB onto MWCNT/ZrO_2/Pb-NCs adsorbent (**Fig. 11**) under are specified following according's: pH = 6.0, 15 min stirring with 0.05 g MWCNT/ZrO_2/Pb-NCs which according supply 95.00% AB and EB removal at C_0 = 15 mg L^{-1} for each dyes. Replication of five confirmation experiments at selected optimal above levels of the process parameters and subsequently according to well-known t-test experimental and predicted values are compared to justify real application of suggested optimum conditions. The adsorption percentages obtained through confirmation experiments are within 94 % of predicted values and as expected these optimal values are valid within the specified range of process parameters. condition of similar experiments over rotational space reveal application of extrapolation/interpolation to predict real behavior of system.

Preprints (www.preprints.org) | NOT PEER-REVIEWED | Posted: 3 February 2021 doi:10.20944/preprints202102.0118.v1

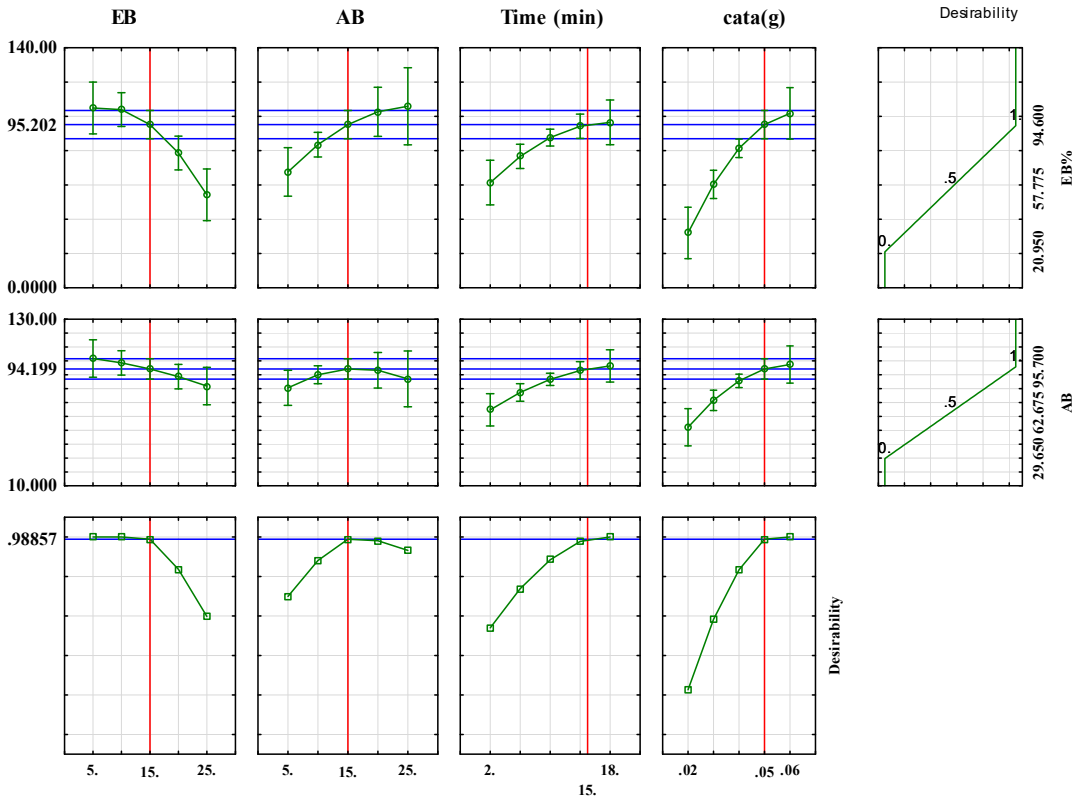

Fig. 11. Optimization plot for the removal of two dyes by MWCNT/ZrO_2/Pb-NCs.

3.7. Equilibrium isotherm study

The adsorption isotherm generally is able to define f the adsorption process among liquid and solid phases following achievement of equilibrium state. The Langmuir, Temkin, Freundlich and Dubinin–Radushkevich models were selected to fit the equilibrium data according to batch adsorption experiments by varying the initial concentration of both dyes over concentration of 1 to 25 mg L^{-1}.

According to correlation coefficient (R^2) correspond **(Table 3)** adsorption of AB and EB onto MWCNT/ZrO_2/Pb -NCs efficiency follow the Langmuir isotherm model with the maximum monolayer adsorption capability of 15.46, 16.92 mg g^{-1} respectively. This result indicates that AB and EB molecules form monolayer coverage on the prepared MWCNT/ZrO_2/Pb –NCs denote homogenous nature of process adsorbent. This also means that every adsorption sites of the MWCNT/ZrO_2/Pb -NCs have the same adsorption energy which the K_L (the energy constant related to the heat of adsorption) value was calculated to be 4.01 and 20.37 L mg^{-1}, respectively.

Table. 3. Isotherm constants Elovich for adsorption of Amido black and Eosin B dyes by MWCNT/ZrO_2/Pb-NCs.

Isotherm	Parameters	Amido black	Eosin B
Langmuir	Qm (mg.g^{-1})	15.46	16.92
	K_L (L mg^{-1})	4.01	20.37
	R^2	0.947	0.985
	R_L	0.04-0.12	0.038-0.21
Freundlich	n	2.21	2.62
	K_F (L mg^{-1})	2.90	3.56

Preprints (www.preprints.org) | NOT PEER-REVIEWED | Posted: 3 February 2021 doi:10.20944/preprints202102.0118.v1

	R^2	0.999	0.994
Temkin	B_1	1.794	2.559
	K_T(L mg^{-1})	16.185	17.303
	R^2	0.8191	0.9823
Dubinin-radushkevich	Qs (mg g^{-1})	9.16	16.52
	β	-10^{-8}	-10^{-8}
	E (kJ mol^{-1})	-7072.1	7072.1
	R^2	0.8963	0.9727

3.8. Kinetic analyses

Adsorption kinetics is basic step to follow and analysis adsorption systems and also to search its optimum operating conditions correspond to accumulation of AB and EB onto 0.05 g of MWCNT/ZrO_2/Pb –NCs under following experimental conditions like at 15 mg L^{-1} of each dyes at pH of around 6.0 and 25 °C. **Table 4** listed different kinetic parameters of the pseudo-first and second-order rate model, Intraparticle diffusion and Elovich for –under study adsorption, the R^2 for the pseudo-second-order kinetic model was found to be higher (> 0.990) along closeness of calculated q_e values ($q_{e,cal}$) to experimental data ($q_{e,exp}$) reveal high efficiency of this model well presentation of real data (see **Table 4**). The intra-particle diffusion rate constants could be obtained from the slopes of the q_t versus $t^{1/2}$ plots (not seen) and were given in **Table 4**. As seen in the table, the plots were linear over the whole time range but possessed linear portions, indicating the not existence of two or more successive steps influenced on the adsorption process.

Table. 4. The first, second order Pseudo kinetics, Intraparticle diffusion and Elovich for adsorption of Amido black and Eosin B dyes by MWCNT/ZrO_2/Pb-NCs.

Model		Amido black	Eosin B
First-order- kinetic	k_1 (min^{-1})	0.195	0196
	$q_{e\ (calc)}$ (mg g^{-1})	9.094	12.64
	R^2	0.978	0.946
Pseudo-second-order-kinetic	k_2 (min^{-1})	0.0153	0.010
	$q_{e\ (calc)}$ (mg g^{-1})	11.33	14.00
	R^2	0.991	0.995
	h (mg g^{-1}min^{-1})	1.950	1.960
Intraparticle diffusion	K_{diff} (mg g^{-1} min$^{-1/2}$)	2.023	2.395
	C (mg g^{-1})	0.431	0.225
	R^2	0.948	0.981
Elovich	β (mg g^{-1} min^{-1})	0.393	0.334
	R^2	0.988	0.987
Experimental data	$q_{e\ (exp)}$ (mg g^{-1})	8.717	10.379

3.9. Reusability of adsorbent

The effect of recycling times of MWCNT/ZrO_2/Pb-NCs on adsorption performance was repeated four times, and the results were illustrated in **Fig. 12**. The adsorption experiments were performed at pH 6.0 and 25 °C. 50 mL of 15 mg L^{-1} dyes solution was used, and the adsorbent mass was 0.05 g per experiment. After each adsorption experiment, the adsorbent was collected by centrifuged, recovered by 5 mL mixture of ethanol: water, then dried and reused. **Fig. 12** showed that the removal efficiency of each dyes was still over 80% after reusing two cycles, indicating that MWCNT/ZrO_2/Pb-NCs had good reusability, and the decrease of the removal efficiency may be result from some irreversible adsorption on the active sites of the adsorbent during the regeneration process.

Preprints (www.preprints.org) | NOT PEER-REVIEWED | Posted: 3 February 2021 doi:10.20944/preprints202102.0118.v1

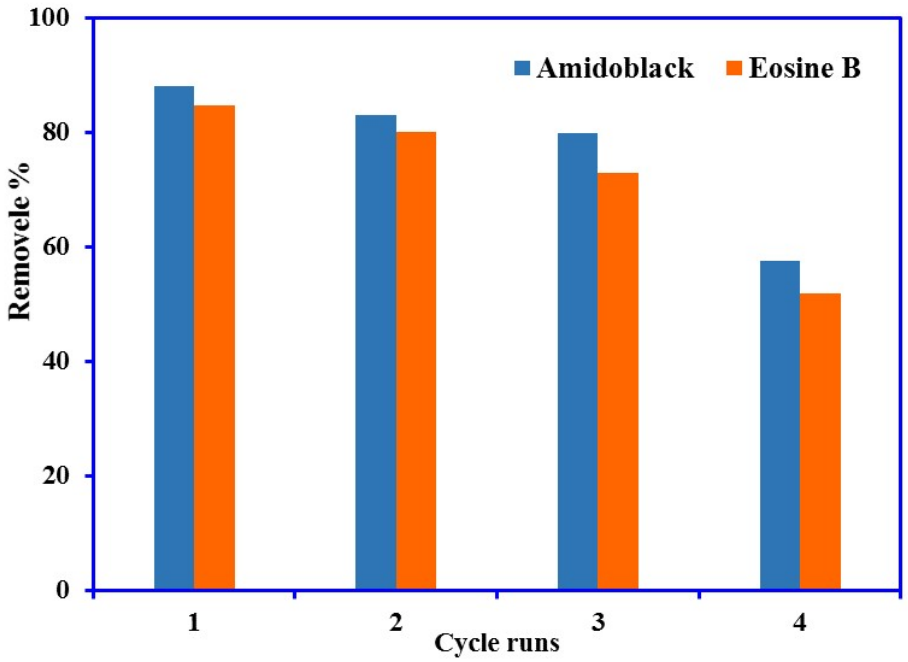

Fig. 12. Effect of reuse cycles on the adsorption efficiency (%) of Amido black and Eosine B onto MWCNT/ZrO_2/Pb-NCs.

4. Conclusions

Multi-walled carbon nanotubes (MWCNT)/ZrO_2/Pb nanocomposites (MWCNT/ZrO_2/Pb-NCs) were fabricated through a facile method and their application as excellent adsorbents for Amido black and Eosin B dyes removal were also demonstrated. The characteristics results of FTIR, FESEM, and XRD showed that MWCNT/ZrO_2/Pb-NCs was successfully prepared. Response surface methodology (RSM) based on four-variable-five-level CCD was employed to interpret the adsorption characteristics of dyes onto MWCNT/ZrO_2/Pb-NCs. The adsorption kinetics, isotherms and thermodynamics were investigated to indicate that the kinetics and equilibrium adsorptions were well-described by pseudo-second-order kinetic and Langmuir isotherm model, respectively. The inherent advantages of the nano-structured adsorbent, such as adsorption capacity, easy, handy operation, rapid extraction, and regeneration, may pave a new, efficient and sustainable way towards highly-efficient dyes removal in water and wastewater treatment.

Acknowledgements

The authors would gratefully acknowledge the financial support of the Mahshahr Branch, Islamic Azad University, Mahshahr, Iran.

References

1. Li, K.; Li, P.; Cai, J.; Xiao, S.; Yang, H.; Li, A., Efficient adsorption of both methyl orange and chromium from their aqueous mixtures using a quaternary ammonium salt modified chitosan magnetic composite adsorbent. *Chemosphere* **2016,** 154, 310-8.

2. Quinlan, P. J.; Tanvir, A.; Tam, K. C., Application of the central composite design to study the flocculation of an anionic azo dye using quaternized cellulose nanofibrils. *Carbohydrate polymers* **2015,** 133, 80-9.

3. Chieng, H. I.; Lim, L. B.; Priyantha, N., Enhancing adsorption capacity of toxic malachite green dye through chemically modified breadnut peel: equilibrium, thermodynamics, kinetics and regeneration studies. *Environmental technology* **2015,** 36, (1-4), 86-97.

4. Garg, V. K.; Gupta, R.; Bala Yadav, A.; Kumar, R., Dye removal from aqueous solution by adsorption on treated sawdust. *Bioresour. Technol.* **2003,** 89, (2), 121-124.

5. Sun, D.; Zhang, X.; Wu, Y.; Liu, X., Adsorption of anionic dyes from aqueous solution on fly ash. *Journal of Hazardous Materials* **2010,** 181, (1), 335-342.

6. Du, W. L.; Xu, Z. R.; Han, X. Y.; Xu, Y. L.; Miao, Z. G., Preparation, characterization and adsorption properties of chitosan nanoparticles for eosin Y as a model anionic dye. *Journal of Hazardous Materials* **2008,** 153, (1–2), 152-156.

7. Arabkhani, P.; Asfaram, A., Development of a novel three-dimensional magnetic polymer aerogel as an efficient adsorbent for malachite green removal. *Journal of Hazardous Materials* **2020,** 384, 121394.

8. Zhang, S. H.; Yang, Q.; Zhou, X.; Li, Z.; Wang, W. J.; Zang, X. H.; Wang, C.; Shiddiky, M. J. A.; Murugulla, A. C.; Nguyen, N. T.; Wang, Z.; Yamauchi, Y., Synthesis of nanoporous poly-melamine-formaldehyde (PMF) based on Schiff base chemistry as a highly efficient adsorbent. *The Analyst* **2019,** 144, (1), 342-348.

9. Vergis, B. R.; Kottam, N.; Krishna, R. H.; Nagabhushana, B., Removal of Evans Blue dye from aqueous solution using magnetic spinel ZnFe2O4 nanomaterial: Adsorption isotherms and kinetics. *Nano-Structures & Nano-Objects* **2019,** 18, 100290.

10. Luan, J.; Hou, P.-X.; Liu, C.; Shi, C.; Li, G.-X.; Cheng, H.-M., Efficient adsorption of organic dyes on a flexible single-wall carbon nanotube film. *Journal of Materials Chemistry A* **2016,** 4, (4), 1191-1194.

11. Duman, O.; Tunc, S.; Polat, T. G.; Bozoglan, B. K., Synthesis of magnetic oxidized multiwalled carbon nanotube-kappa-carrageenan-Fe3O4 nanocomposite adsorbent and its application in cationic Methylene Blue dye adsorption. *Carbohydrate polymers* **2016,** 147, 79-88.

12. Krishna Kumar, A. S.; Jiang, S.-J.; Tseng, W.-L., Effective adsorption of chromium(vi)/Cr(iii) from aqueous solution using ionic liquid functionalized multiwalled carbon nanotubes as a super sorbent. *Journal of Materials Chemistry A* **2015,** 3, (13), 7044-7057.

13. Yang, Q.; Chen, G.; Zhang, J.; Li, H., Adsorption of sulfamethazine by multi-walled carbon nanotubes: effects of aqueous solution chemistry. *RSC Advances* **2015,** 5, (32), 25541-25549.

14. Unsal, Y. E.; Soylak, M.; Tuzen, M., Spectrophotometric Detection of Rhodamine B after Separation-Enrichment by Using Multi-walled Carbon Nanotubes. *Journal of AOAC International* **2014,** 97, (5), 1459-62.

15. Gusain, R.; Kumar, N.; Fosso-Kankeu, E.; Ray, S. S., Efficient Removal of Pb(II) and Cd(II) from Industrial Mine Water by a Hierarchical MoS2/SH-MWCNT Nanocomposite. *ACS Omega* **2019,** 4, (9), 13922-13935.

16. Yang, R. L.; Zheng, Y. P.; Wang, T. Y.; Li, P. P.; Wang, Y. D.; Yao, D. D.; Chen, L. X., Solvent-free nanofluid with three structure models based on the composition of a MWCNT/SiO2 core and its adsorption capacity of CO2. *Nanotechnology* **2018,** 29, (3), 035704.

17. Mallakpour, S.; Rashidimoghadam, S., Starch/MWCNT-vitamin C nanocomposites: Electrical, thermal properties and their utilization for removal of methyl orange. *Carbohydrate polymers* **2017,** 169, 23-32.

18. Shirmardi, M.; Mesdaghinia, A.; Mahvi, A. H.; Nasseri, S.; Nabizadeh, R., Kinetics and equilibrium studies on adsorption of acid red 18 (Azo-Dye) using multiwall carbon nanotubes (MWCNTs) from aqueous solution. *Journal of Chemistry* **2012,** 9, (4), 2371-2383.

19. Gabal, M.; Al-Harthy, E.; Al Angari, Y.; Salam, M. A., MWCNTs decorated with $Mn_{0.8}Zn_{0.2}Fe_2O_4$ nanoparticles for removal of crystal-violet dye from aqueous solutions. *Chemical Engineering Journal* **2014,** 255, 156-164.

20. Zhao, D.; Zhang, W.; Chen, C.; Wang, X., Adsorption of methyl orange dye onto multiwalled carbon nanotubes. *Procedia Environmental Sciences* **2013,** 18, 890-895.

21. Wang, S.; Ng, C. W.; Wang, W.; Li, Q.; Hao, Z., Synergistic and competitive adsorption of organic dyes on multiwalled carbon nanotubes. *Chemical Engineering Journal* **2012,** 197, 34-40.

22. Bajpai, S.; Gupta, S. K.; Dey, A.; Jha, M. K.; Bajpai, V.; Joshi, S.; Gupta, A., Application of Central Composite Design approach for removal of chromium (VI) from aqueous solution using weakly anionic resin: modeling, optimization, and study of interactive variables. *J. Hazard. Mater.* **2012,** 227-228, 436-44.

23. Lingamdinne, L. P.; Koduru, J. R.; Chang, Y. Y.; Karri, R. R., Process optimization and adsorption modeling of Pb(II) on nickel ferrite-reduced graphene oxide nano-composite. *Journal of Molecular Liquids* **2018,** 250, 202-211.

24. Alipanahpour Dil, E.; Ghaedi, M.; Asfaram, A.; Mehrabi, F.; Sadeghfar, F., Efficient adsorption of Azure B onto CNTs/Zn:ZnO@Ni_2P-NCs from aqueous solution in the presence of ultrasound wave based on multivariate optimization. *Journal of Industrial and Engineering Chemistry* **2019,** 74, 55-62.

25. Sadeghfar, F.; Ghaedi, M.; Asfaram, A.; Jannesar, R.; Javadian, H.; Pezeshkpour, V., Polyvinyl alcohol/Fe_3O_4@carbon nanotubes nanocomposite: Electrochemical-assisted synthesis, physicochemical characterization, optical properties, cytotoxicity effects and ultrasound-assisted treatment of aqueous based organic compound. *Journal of Industrial and Engineering Chemistry* **2018,** 65, 349-362.

26. Asfaram, A.; Ghaedi, M.; Dashtian, K.; Ghezelbash, G. R., Preparation and Characterization of Mn0.4Zn0.6Fe2O4 Nanoparticles Supported on Dead Cells of Yarrowia lipolytica as a Novel and Efficient Adsorbent/Biosorbent Composite for the

Removal of Azo Food Dyes: Central Composite Design Optimization Study. *ACS Sustainable Chemistry and Engineering* **2018,** 6, (4), 4549-4563.

27. Asfaram, A.; Ghaedi, M.; Yousefi, F.; Dastkhoon, M., Experimental design and modeling of ultrasound assisted simultaneous adsorption of cationic dyes onto ZnS: Mn-NPs-AC from binary mixture. *Ultrasonics sonochemistry* **2016,** 33, 77-89.

28. Yang, Y.; Yu, W.; He, S.; Yu, S.; Chen, Y.; Lu, L.; Shu, Z.; Cui, H.; Zhang, Y.; Jin, H., Rapid adsorption of cationic dye-methylene blue on the modified montmorillonite/graphene oxide composites. *Applied Clay Science* **2019,** 168, 304-311.

29. Bazrafshan, A. A.; Ghaedi, M.; Hajati, S.; Naghiha, R.; Asfaram, A., Synthesis of ZnO-nanorod-based materials for antibacterial, antifungal activities, DNA cleavage and efficient ultrasound-assisted dyes adsorption. *Ecotoxicology and Environmental Safety* **2017,** 142, 330-337.

30. Asfaram, A.; Ghaedi, M.; Yousefi, F.; Dastkhoon, M., Experimental design and modeling of ultrasound assisted simultaneous adsorption of cationic dyes onto ZnS: Mn-NPs-AC from binary mixture. *Ultrason. Sonochem.* **2016,** 33, 77-89.

31. Machado, F. M.; Bergmann, C. P.; Fernandes, T. H. M.; Lima, E. C.; Royer, B.; Calvete, T.; Fagan, S. B., Adsorption of Reactive Red M-2BE dye from water solutions by multi-walled carbon nanotubes and activated carbon. *Journal of Hazardous Materials* **2011,** 192, (3), 1122-1131.

32. Mourabet, M.; El Rhilassi, A.; El Boujaady, H.; Bennani-Ziatni, M.; El Hamri, R.; Taitai, A., Removal of fluoride from aqueous solution by adsorption on hydroxyapatite (HAp) using response surface methodology. *Journal of Saudi Chemical Society* **2015,** 19, (6), 603-615.

1